

Error-Correcting Neural Network

Yang Song, Qiyu Kang, and Wee Peng Tay

Abstract

Error-correcting output codes (ECOC) is an ensemble method combining a set of binary classifiers for multi-class learning problems. However, in traditional ECOC framework, the binary classifiers are trained independently. To explore the interaction between the binary classifiers, we construct an error correction network (ECN) that jointly trains all binary classifiers while maximizing the ensemble diversity to improve its robustness against adversarial attacks. An ECN is built based on a code matrix which is generated by maximizing the error tolerance, i.e., the minimum Hamming distance between any two rows, as well as the ensemble diversity, i.e., the variation of information between any two columns. Though ECN inherently promotes the diversity between the binary classifiers as each ensemble member solves a different classification problem (specified by the corresponding column of the code matrix), we empirically show that the ensemble diversity can be further improved by forcing the weight matrices learned by ensemble members to be orthogonal. The ECN is trained in end-to-end fashion and can be complementary to other defense approaches including adversarial training. We show empirically that ECN is effective against the state-of-the-art while-box attacks while maintaining good accuracy on normal examples.

I. INTRODUCTION

Deep learning has been widely and successfully applied in many tasks such as imaging classification [1], [2], speech recognition [3], and natural language processing [4]. However, recent works [5] noticed the existence of adversarial examples in the image classification tasks. The original images can be perturbed such that perturbation is human imperceptible but the deep neural networks (DNNs) will be fooled to mis-classify.

To mitigate the effect of adversarial attacks, many defences have been proposed. Generally speaking, these defence methods fall into three (mutually compatible) categories:

The authors are with the School of Electrical and Electronic Engineering, Nanyang Technological University, Singapore. E-mails: songy@ntu.edu.sg, KANG0080@e.ntu.edu.sg, wptay@ntu.edu.sg. Yang Song and Qiyu Kang contribute equally to this work.

- 1) adversarial training, which augments the training data with adversarial examples [5], [6],
- 2) modifying neural network/training procedure, e.g., defensive distillation [7], and
- 3) post-training defences, which attempt to remove the adversarial noise from the input examples [8]–[10] in the testing phase.

Our method belongs to type 2 defence. While most of the defences of this type focus on robustifying a single network, there some works have considered using ensemble models [11]–[13]. The ensemble members solve the same classification problem, thus it is essential to promote the diversity among the ensemble members to prevent adversarial examples from transferring between them, i.e., the adversarial examples crafted for one member may also fool the other members thus making the ensemble model ineffective defending adversarial examples. ECOC [14], [15] is a special ensemble model that combines a set of binary classifiers according to a given code matrix. In its applications to sensor networks [16], [17] and crowdsourcing systems [18], [19] where sensors or crowd workers act as unreliable binary classifiers, ECOC has shown its fault-tolerant capacity in such harsh scenarios. Our proposed ECN is inspired by the significant fault-tolerant ability of ECOC.

The ECN is constructed based on a binary code matrix where each row of the code matrix is a N -bit codeword representing one class label. Given a codeword length N and number of classes L , a code matrix is generated in an iterative manner with the objective of maximizing the minimum distance between any two rows and that between any two columns. Let ECN_N denote an ECN with each class label being encoded into N bits. A simple example can be found in Table I. Each column of a code matrix groups the original L classes into two *macro-*

TABLE I
EXAMPLE OF ECN_4 WHILE THERE ARE $L = 3$ CLASSES.

| Class | Net 1 | Net 2 | Net 3 | Net 4 |
|-------|-------|-------|-------|-------|
| 1 | 1 | 0 | 1 | 0 |
| 2 | 1 | 1 | 0 | 1 |
| 3 | 0 | 0 | 0 | 1 |

classes with macro-class 0 containing classes indicated by bit 0 and macro-class 1 containing classes indicated by bit 1, and thus ECN consists of N binary classifiers aiming for different tasks. The central idea is ECN creates sufficient redundancy in the codewords such that it may tolerate some wrong predictions, i.e., flipped bits, made by individual networks. ECN

promotes the diversity between models by design as its members are working for different binary classification tasks. Thus, adversarial examples crafted for one individual network has less impact [20] on the other members as compared to the existing ensemble model whose members are working on the same task. To explore the interaction between ensemble members, we promote the orthogonality between the weight matrices learned at the last layer of the members. After all individual networks make their binary predictions, we concatenate them into a N -bit predicted codeword and use a decoder (a trainable dense layer) to make the final prediction. In sum, we obfuscate deliberately in each binary classifier the training labels by partitioning them into two macro-classes, and in the final layer of ECN, the original L labels are decoded via a trainable dense layer, thereby ECN can be trained in end-to-end fashion.

Our main contributions are summarized below

- 1) We apply the idea of error correction codes in building a neural network to improve model's adversarial robustness and show how this neural network can be trained in end-to-end fashion.
- 2) We extensively study (by experiments) the impact of code matrix on the adversarial robustness of ECN and relate row distance to error tolerance and column distance to ensemble diversity and suggest to optimize both distances for better robustness.
- 3) We show combining ECN with adversarial training further improves model robustness.
- 4) We extend binary ECN to q -ary ECN where its branches are q -ary classifiers with $q \geq 2$ and study its robustness against the binary case.
- 5) We show how to adapt ECN to sparse code matrix.

In experiments, we test ECN on two widely used dataset MNIST [21] and CIFAR-10 [22] under several well-known adversarial attacks. The results show that ECN significantly improves the robustness against adversarial examples. The rest of this paper is organized as follows. In Section II, we brief the well-known adversarial attacks. In Section III, we introduce the structure and the training strategy of our ECN. In Section IV, we present extensive experiments results. Section V concludes the paper.

II. ATTACK METHODS

For a normal image-label pair (x, y) and a trained DNN f_θ with θ being trained model parameter, adversarial attacks attempt to find an adversarial example x' that remains in the L_p -ball of radius ϵ centered at the normal example x , i.e., $\|x - x'\|_p \leq \epsilon$, such that $f_\theta(x') \neq y$.

In what follows, we brief some popular adversarial attacks which will be used to verify our proposed ECN.

Fast Gradient Sign Method (FGSM) [6] perturbs a normal image x in its L_∞ neighbourhood to get x'

$$x' = x + \epsilon \cdot \text{sign}(\nabla_x \mathcal{L}(f_\theta(x), y)),$$

where $\mathcal{L}(f_\theta(x), y)$ is the cross-entropy loss of classifying x as label y , and ϵ denotes perturbation magnitude, and update direction at each pixel is determined by the sign of the gradient evaluated at this pixel. FGSM is a simple yet fast and powerful attack.

Basic Iterative Method (BIM) [23] iteratively refines the FGSM by taking multiple smaller steps α in the direction of gradient-sign. The refinement at iteration i takes the form below

$$x'_i = x'_{i-1} + \text{clip}_{\epsilon, x}(\alpha \cdot \text{sign}(\nabla_x \mathcal{L}(f_\theta(x), y))),$$

where $x'_0 = x$ and $\text{clip}_{\epsilon, x}(x')$ performs per-pixel clipping of the image x' . For example, if pixel takes value between 0 and 255, $\text{clip}_{\epsilon, x}(x') = \min\{255, x + \epsilon, \max\{0, x - \epsilon, x'\}\}$.

Projected Gradient Descent (PGD) [24] has the same generation process as BIM except PGD starts the gradient descent from a point x'_0 chosen uniformly at random in the L_∞ -ball of radius ϵ centered at x .

Jacobian-based Saliency Map Attack (JSMA) [25] is a greedy algorithm that adjusts one pixel at a time. Given a target label t , JSMA computes a saliency map at pixels $(p, q), p \in \{1, \dots, P\}, q \in \{1, \dots, Q\}$ of image x

$$S(p, q) = -\alpha_{p,q} \cdot \beta_{p,q} \cdot (\alpha_{p,q} > 0) \cdot (\beta_{p,q} < 0),$$

where $\alpha_{p,q} = \frac{\partial Z(x,t)}{\partial x_{p,q}}$ and $\beta_{p,q} = \sum_{j \neq t} \frac{\partial Z(x,j)}{\partial x_{p,q}}$ and $Z(x, i)$ denotes the logit associated with label i . The logits are the inputs to the softmax function. A large value of $S(p, q)$ indicates pixel (p, q) has big impact on labelling x as t . Let $(p^*, q^*) = \arg \max_{p,q} S(p, q)$. Then, $x_{p^*, q^*} = \min(\text{clip}_{\max}, x_{p,q} + \theta)$. This process repeats until either misclassification happens or it reaches the maximum iterations which equals to $\lfloor \frac{\gamma \cdot PQ}{2} \rfloor$. Note that JSMA is a targeted attack by design and its untargeted attack selects the target class at random.

Carlini & Wagner (C&W) [26]: Here, we consider C&W L_2 attack only. Let $x' = x +$

$\frac{1}{2}(\tanh(\omega) + 1)$. For a normal example (x, y) , C&W finds the perturbation by solving the following optimization problem

$$\min_{\omega} \left\| \frac{1}{2}(\tanh(\omega) + 1) - x \right\|_2^2 + c \cdot \ell \left(\frac{1}{2}(\tanh(\omega) + 1) \right),$$

where $\ell(x') = \max(Z(x', y) - \max\{Z(x', i) : i \neq y\} + \kappa, 0)$. Large confidence parameter κ encourages misclassification.

III. ERROR-CORRECTING NEURAL NETWORK

In this section, we detail the structure of ECN and its training strategy. The way of generating code matrix is also briefed.

A. Error Correcting Code

Hamming distance is an important measure in error detection. It determines the maximum number of bits that is allowed to flip in one codeword without confusing it with the other codeword. Adding more bits to the codewords can increase the Hamming distance. A good error detecting code is to be able to maximize the minimum Hamming distance between any two codewords. Let r_i be the i -th codeword of code matrix \mathbf{M} , and $H(r_i, r_j)$ be the Hamming distance between the i -th and j -th codewords of code matrix \mathbf{M} , i.e., the number of bits positions where they differ. The minimum Hamming distance of code matrix \mathbf{M} is then given by $d_H(\mathbf{M}) = \min_{i \neq j} H(r_i, r_j)$. In principle, in channel communications, if we decode the received message to the class whose codeword has the minimum Hamming distance to the received message, a code matrix \mathbf{M} can always decode correctly a message with up to $d_H(\mathbf{M})/2$ erroneous bits. For example, a code matrix with minimum Hamming distance 2 can correct one erroneous bit.

B. Error Correcting Network

ECN combines an encoder and a decoder as shown in Fig. 1, where the encoder consists of N parallel neural networks, i.e., binary classifiers, and the decoder, acting as a fusion center, is built based on the generated code matrix \mathbf{M} .

Encoder: Given a code matrix \mathbf{M} of $\{0, 1\}$ of size $L \times N$, each column of \mathbf{M} groups L classes into two classes: all 1's belong to macro-class 1 and all 0's belong to the other macro-class 0. There are N binary classifiers, each of which is a convolutional neural network (CNN), taking the same images as their inputs. The n -th CNN outputs two probabilities $\{P_{0,n}, P_{1,n}\}, n = 1, \dots, N$

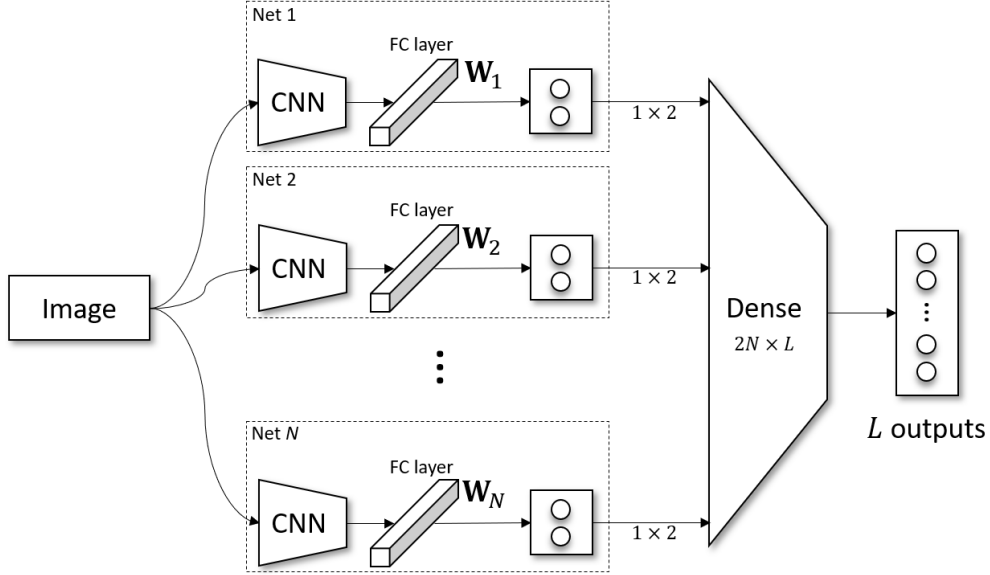


Fig. 1. ECN architecture.

(at the softmax layer) corresponding to macro-class 0 and macro-class 1. In addition, we extract the features from the second-to-last layer of each CNN and scale them via a batch norm layer. These features, $\{\mathcal{F}_1, \dots, \mathcal{F}_N\}$, will be used to measure the diversity between the individual CNNs.

Decoder: ECN makes predictions through a decoder which returns a label whose codeword (defined by code matrix) matches the predicted codeword (encoder's output) the best. Here, we consider two decoder options.

- 1) Decoder 1: Fig. 2a shows its architecture. We extract the prediction probabilities corresponding to class "1", i.e., $P_{1,n}, n = 1, \dots, N$, and stack them into a vector $\mathbf{p}_1 = [P_{1,1}, \dots, P_{1,N}]$. Scaling the values of \mathbf{p}_1 from $[0, 1]$ to $[-1, 1]$ results in $\bar{\mathbf{p}}_1 = 2\mathbf{p}_1 - 1$. Then, we mix $\bar{\mathbf{p}}_1$ with the transpose of the code matrix, $\bar{\mathbf{M}}^T$, where $\bar{\mathbf{M}} = 2\mathbf{M} - 1$. If the prediction accuracy is high for each binary classifier, the entries in $\bar{\mathbf{p}}_1$ will take values either close to 1 or close to -1, and thus the larger entries in $\bar{\mathbf{p}}_1 \bar{\mathbf{M}}^T$ indicate better matching between $\bar{\mathbf{p}}_1$ and the columns of $\bar{\mathbf{M}}$.
- 2) Decoder 2: Fig. 2b shows its architecture. As discussed in decoder 1, it is not optimal to mix $\bar{\mathbf{p}}_1$ of values in $[-1, 1]$ with $\bar{\mathbf{M}}$ of values $\{-1, 1\}$. To accommodate the continuous inputs (to the dense layer), we use a trainable dense layer Φ . As all binary classifiers are defined by the code matrix \mathbf{M} , simultaneously maximizing the classification accuracy of

each binary classifier (the inputs to Φ) and that of the L -class classifier (the output of Φ) will force Φ to reconstruct $\bar{\mathbf{M}}$. Fig. 3 gives such an example. We generate a code matrix \mathbf{M} with $L = 10, N = 20$, and Fig. 3b shows Φ obtained after training on MNIST data using decoder 2 where Φ_E contains the even rows of Φ , and Fig. 3c shows $\text{sign}(\Phi)$ is same as $\bar{\mathbf{M}}$ except for few entries that are flipped.

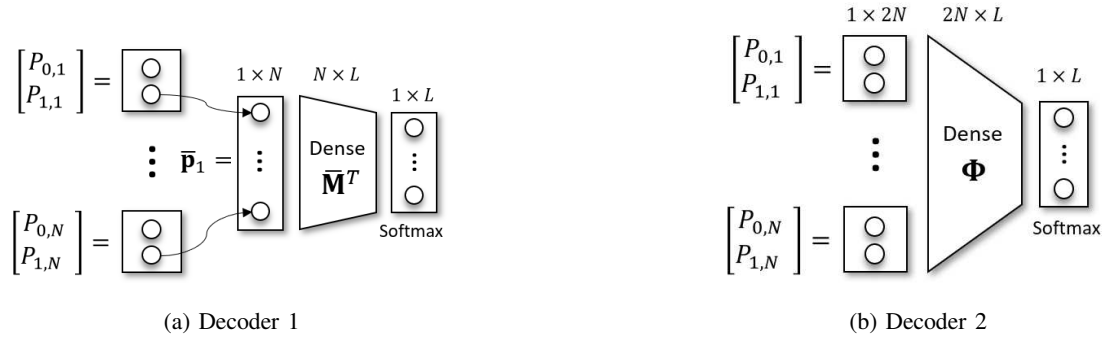


Fig. 2. Architectures of two decoder options.

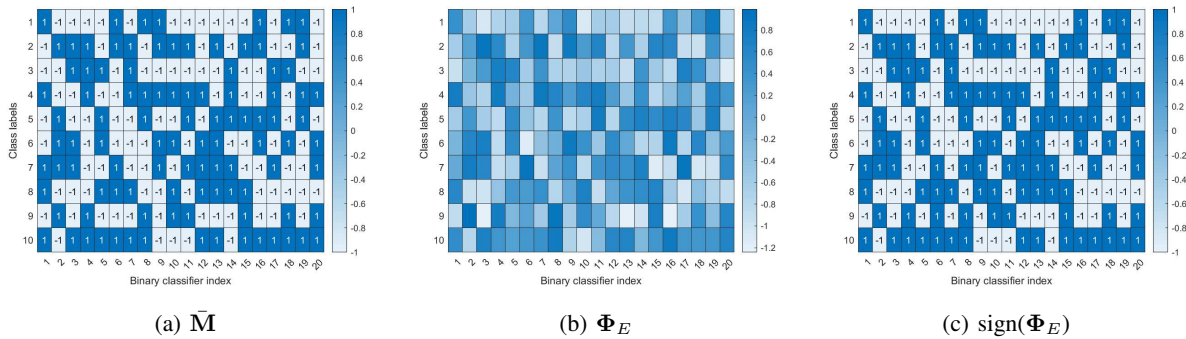


Fig. 3. Reconstruction of $\bar{\mathbf{M}}$ from Φ_E , where Φ_E denotes a matrix containing the even rows of Φ .

Diversity promoting between models: We impose orthogonality between the weight matrices, $\mathbf{W}_1, \dots, \mathbf{W}_N$, learned at the last layer by all ensemble members with the objective of increasing diversity between individual neural networks. After normalizing the columns of $\mathbf{W}_1, \dots, \mathbf{W}_N$ under L_2 -norm, the ensemble diversity can be defined by

$$\mathcal{D} = \sum_{i < j} |\mathbf{W}_i^T \mathbf{W}_j|, \quad 1 \leq i < j \leq N,$$

where $|\cdot|$ returns the sum of absolute values of all matrix entries.

Ensemble loss: Given a image-label pair (x, y) , the overall loss function combines the ensemble

cross-entropy $\mathcal{L}_{\text{CE}}(x, y)$, average of the individual cross-entropies $\mathcal{L}_{\text{CE}}^{(n)}(x, y, [\mathbf{M}]_n), \forall n$ and the diversity promoting regularizer $\mathcal{D}(x)$:

$$\mathcal{L}_{\text{ECN}}(x, y) \tag{1}$$

$$= \mathcal{L}_{\text{CE}}(x, y) + \frac{\alpha}{N} \sum_{n=1}^N \mathcal{L}_{\text{CE}}^{(n)}(x, y, [\mathbf{M}]_n) - \beta \mathcal{D}(x), \tag{2}$$

$$= -\mathbf{1}_y^\top \log(\mathbf{p}(x)) + \frac{\alpha}{N} \sum_{n=1}^N -\mathbf{1}_{y^{(n)}}^\top \log(\mathbf{p}^{(n)}(x)) - \beta \mathcal{D}(x), \tag{3}$$

where $\mathbf{1}_y$ is a L -dimensional one-hot encoding of y and $\mathbf{1}_{y^{(n)}}$ is a 2-dimensional one-hot encoding of $y^{(n)}$ which is a binary label obtained by partitioning the L -ary label y into two macro-classes according the n -th column of \mathbf{M} , i.e., $[\mathbf{M}]_n$, $\mathbf{p}(x)$ contains the L -class probabilities obtained by passing x through the entire ECN and $\mathbf{p}^{(n)}(x)$ contains the 2-class probabilities obtained by passing x through the n -th binary classifier, and $\alpha, \beta \geq 0$.

Code matrix design: As we have mentioned in Section III-A, a code matrix with larger $d_H(\mathbf{M})$ is preferred since it can correct more errors, resulting a better classification performance. However, if we only consider maximizing $d_H(\mathbf{M})$ when designing code matrix, the two columns of the matrix may lead the corresponding two binary classifiers to perform the same classification task even they have different bits. For a concrete illustration, consider again the code matrix example in Table I. The last two columns in Table I are different, while Net 3 and Net 4 are essentially performing the same task: classifying the classes to set $\{1\}$ or $\{3, 4\}$. A adversarial example targeting at fooling Net 3 is expected to has the transferability to fool Net 4 simultaneously, weakening the robustness of ECN. To further promote the diversity between the individual classification networks, we therefore include the column diversity when designing the code matrix. Specifically, we view each column of the code matrix as partitioning the L -classes into clusters, and measure the difference between two columns using Variation of Information (VI) metric [27]. VI is a criterion for comparing the difference between two q -ary partitions, measuring the amount of information lost and gained in changing from one clustering to another clustering [27]. ECN shown above focuses on the binary individual classifier with each column of the code matrix being a binary cluster. A natural extension is the general q -ary code matrix with each ensemble member performing a q -ary classification problem. We denote the m -th column of code matrix \mathbf{M} as c_m , the classes belongs to macro-class k in the n -th column as c_n^k , where

$m = 1, \dots, N$ and $k = 0, \dots, q - 1$. The VI distance defined in [27] between c_m and c_n is:

$$\begin{aligned}
 VI(c_m, c_n) = & - \sum_{k=0}^{q-1} s_m(k) \log s_m(k) - \sum_{k'=0}^{q-1} s_n(k') \log s_n(k') \\
 & - 2 \sum_{k=0}^{q-1} \sum_{k'=0}^{q-1} s_{m,n}(k, k') \log \frac{s_{m,n}(k, k')}{s_m(k) s_n(k')},
 \end{aligned} \tag{4}$$

where $s_{m,n}(k, k') = \frac{|c_m^k \cap c_n^{k'}|}{L}$, $s_m(k) = \frac{|c_m^k|}{L}$ and $s_n(k') = \frac{|c_n^{k'}|}{L}$. The minimum VI distance of code matrix \mathbf{M} is then given by $d_{VI}(\mathbf{M}) = \min_{m \neq n} VI(c_m, c_n)$.

The code matrix is designed to

$$\max_M d_H(\mathbf{M}) + d_{VI}(\mathbf{M}), \tag{5}$$

which is however a NP-complete problem [28]. We adopt simulated annealing [29], [30] to solve this optimization problem heuristically, where the energy function is set as:

$$\max_M \sum_{i \neq j} H(r_i, r_j) + \sum_{m \neq n} VI(c_m, c_n), \tag{6}$$

instead of (5). This is a common technique used in simulated annealing [30] and is because bit changes not involving the minimum distance pairs would not be reflected in the energy function if it is set as (5). The performances of the generalized q -ary ECN are compared in Section IV-G.

As each of the encoder neural network is assigned with different binary classification task. We believe this technique can force each ensemble member to learn different features, thus reducing the transferability of the adversarial examples among binary classification networks.

IV. EXPERIMENTS

We evaluate the adversarial robustness of ECN under the attack methods introduced in Section II with different attack parameters.

A. Setup

We test on two standard datasets: MNIST [2] and CIFAR10 [31]. For both MNIST and CIFAR10, we select 50,000 examples for the training set and 10,000 examples for the test set, and scale all pixel values from $[0, 255]$ to $[0, 1]$. We use ResNet20 [32] as the baseline for both MNIST and CIFAR10. The baseline can achieve testing accuracy of 99.5% and 90.3% on MNIST and CIFAR10, respectively. For ECN, we consider two neural networks given in Table II as the binary classifier's architecture. The training parameters are given in Table III.

TABLE II
ARCHITECTURE OPTIONS FOR THE INDIVIDUAL NETWORKS.

| Net A | Net B | |
|---------------|---------------|-------------------------|
| ResNet14 [32] | Conv.ReLU | $3 \times 3 \times 64$ |
| | Conv.ReLU | $3 \times 3 \times 64$ |
| | Max Pooling | 2×2 |
| | Dropout | 0.25 |
| | Conv.ReLU | $3 \times 3 \times 128$ |
| | Conv.ReLU | $3 \times 3 \times 128$ |
| | Max Pooling | 2×2 |
| | Dropout | 0.25 |
| | Dense.ReLU | 512 |
| | Dropout | 0.5 |
| | Dense.Softmax | 2 |

TABLE III
TRAINING PARAMETERS.

| Parameters | MNIST | CIFAR10 |
|---------------------|-------|----------------------------|
| Optimization Method | | Adam |
| Batch size | | 128 |
| Epochs | 50 | 200 |
| Data centering | False | True |
| Data Augmentation | False | Shifting + Horizontal Flip |

B. Performance under White-box Attacks

White-box adversaries know all the information about the classifier models, including training data, model architectures and parameters. We test the performance of ECN in defending white-box attacks. Table IV gives the parameters for different attack methods.

We compare our ECN with another ensemble method proposed in [13], namely adaptive diversity promoting (ADP) ensemble method, for which we use the same architecture and model parameters as reported in [13], i.e., $ADP_{2,0.5}$ with three ResNet20 being its ensemble members. Note that the optimal solution of ADP is attained when $L - 1$ is divisible by the number of ensemble members N . For $L = 10$, using $N = 3$ is optimal for ADP and increasing N beyond that will not improve its performance.

The classification results on MNIST are shown in Table V. We can see the ECN significantly

TABLE IV
PARAMETERS OF ATTACK METHODS FOR DIFFERENT DATASETS

| Attack methods | Para. | MNIST | CIFAR10 |
|----------------|--------------------|-------|---------|
| BIM, PGD | iteration size | 20 | 10 |
| | step size | 0.05 | 0.02 |
| JSMA | θ | | 1 |
| | batch size | | 100 |
| C&W | learning rate | 0.00 | |
| | binary search step | | 5 |

improves the adversarial robustness as compared to the baseline and $ADP_{2,0.5}$, especially for the parameters that lead to stronger attack. ECN also maintains state-of-the-art accuracy on normal images. From the last two columns, we can see forcing orthogonality between individual networks' weight matrices is effective in improving the robustness.

Table VI presents results for CIFAR10. ECN is tested using two different binary classifiers. For both options (net A and net B), ECN is consistently more robust than the competitors while the classification accuracy on normal images is slightly lower as compared with $ADP_{2,0.5}$. We believe it is possible to further improve ECN's testing accuracy via a better binary classifier model but it is beyond this paper's scope. When we were constructing a neural network for binary classifiers, we found that batch normalization (BN) causes adversarial vulnerability which can be observed in "w/ BN" and "w/o BN" columns. The model with BN becomes more vulnerable especially under gradient-based attacks, e.g. FGSM, BIM and PGD. This is consistent with what was recently reported in [33] and one possible explanation could be that BN can cause gradient exploding [34].

C. Adversarial Training Based on ECN

ECN is complementary to the other defenses. Here we combine ECN with adversarial training (AdvT), which is the most widely studied defense. Our ECN-based AdvT follows the procedure stated in Algorithm 1. The results in Table VII are obtained using $N = 20, \alpha = 10, \beta = 0$ and net B for ECN and letting $I = 200$ and $B = 10000$, and choosing $\epsilon = 0.04$ for FGSM. From the results, we can see the combination of ECN and AdvT significantly improves the testing accuracy over ECN which implies more robust model makes AdvT more effective.

TABLE V

CLASSIFICATION ACCURACY (%) ON ADVERSARIAL MNIST EXAMPLES. FOR ECN, WE USE $N = 30$ BINARY CLASSIFIERS AND SET $\alpha = 10$.

| Attacks | Para. | Baseline | ADP _{2,0.5} | ECN ₃₀ using net B | |
|---------|------------------|----------|----------------------|-------------------------------|---------------|
| | | | | $\beta = 0$ | $\beta = 0.1$ |
| No att. | - | 99.5 | 99.7 | 99.7 | 99.7 |
| FGSM | $\epsilon = 0.1$ | 93.2 | 97.8 | 98.8 | 98.9 |
| | $\epsilon = 0.2$ | 83.5 | 95.3 | 92.2 | 93.6 |
| | $\epsilon = 0.3$ | 70.5 | 69.1 | 62.2 | 72.7 |
| BIM | $\epsilon = 0.1$ | 3.5 | 46.9 | 98.7 | 98.8 |
| | $\epsilon = 0.2$ | 0.5 | 0.45 | 85.2 | 87.2 |
| | $\epsilon = 0.3$ | 0.5 | 0.18 | 36.6 | 52.3 |
| PGD | $\epsilon = 0.1$ | 0.3 | 47.0 | 98.8 | 98.8 |
| | $\epsilon = 0.2$ | 0.02 | 0.2 | 86.1 | 88.5 |
| | $\epsilon = 0.3$ | 0.01 | 0.01 | 41.1 | 58.0 |
| JSMA | $\gamma = 0.6$ | 1.9 | 7.7 | 82.0 | 87.7 |
| C&W | $\kappa = 1$ | 0.4 | 15.5 | 99.4 | 99.5 |

TABLE VI

CLASSIFICATION ACCURACY (%) ON ADVERSARIAL CIFAR10 EXAMPLES, WHERE "w/o BN" INDICATES THE NET EXCLUDES BATCH NORMALIZATION LAYERS. FOR ECN, WE USE $N = 30$ BINARY CLASSIFIERS AND SET $\alpha = 10$.

| Attacks | Para. | Baseline | ADP _{2,0.5} | | ECN ₃₀ using net A | | ECN ₃₀ using net B | |
|---------|-------------------|----------|----------------------|--------|-------------------------------|--------|-------------------------------|---------------|
| | | | w/ BN | w/o BN | w/ BN | w/o BN | $\beta = 0$ | $\beta = 0.5$ |
| No att. | - | 90.3 | 93.4 | 91.6 | 93.0 | 89.9 | 90.4 | 90.2 |
| FGSM | $\epsilon = 0.04$ | 11.8 | 46.3 | 46.2 | 50.7 | 59.4 | 63.7 | 65.6 |
| BIM | $\epsilon = 0.04$ | 5.9 | 6.13 | 15.1 | 51.8 | 53.8 | 57.9 | 62.2 |
| PGD | $\epsilon = 0.04$ | 4.8 | 5.62 | 13.4 | 53.4 | 55.2 | 59.2 | 63.2 |
| JSMA | $\gamma = 0.2$ | 1.3 | 16.3 | 24.5 | 82.6 | 81.4 | 80.1 | 79.6 |
| C&W | $\kappa = 1$ | 6.4 | 4.56 | 6.3 | 92.4 | 89.0 | 89.8 | 89.7 |

D. ECN vs. Independent Training of Binary Classifiers

ECN explores the interaction between the binary classifiers via a trainable decoder. This is different from conventional ECOC which trains classifiers independently. The advantage of our training procedure is experimentally verified and can be seen in Fig. 4, where ECOC uses Hamming distance to decode.

Algorithm 1 Adversarial training on ECN

Input: A pre-trained ECN denoted as $\text{ECN}_N^{\{0\}}$
Output: $\text{ECN}_N^{\{I_{\max}\}}$ $\{I_{\max}$ indexes the ECN with the best validation accuracy $\}$

- 1: **for** $i = 1, \dots, I$ **do**
 - 2: Randomly select B clean images from the training set and craft their adversarial examples from $\text{ECN}_N^{\{i-1\}}$ using FGSM.
 - 3: Augment training data with B adversarial examples.
 - 4: Train $\text{ECN}_N^{\{i\}}$ from $\text{ECN}_N^{\{i-1\}}$
 - 5: **end for**
-

TABLE VII

 CLASSIFICATION ACCURACY (%) ON ADVERSARIAL CIFAR10 EXAMPLES. FOR ECN, WE USE $N = 20$ NET B BINARY CLASSIFIERS AND SET $\alpha = 10, \beta = 0$.

| Attacks | Para. | Baseline | Baseline + AdvT | ECN | ECN+AdvT |
|---------|-------------------|----------|-----------------|------|-------------|
| No att. | - | 90.26 | 87.8 | 90.1 | 90.3 |
| FGSM | $\epsilon = 0.02$ | 15.5 | 26.9 | 79.3 | 87.6 |
| | $\epsilon = 0.04$ | 11.8 | 22.4 | 60.0 | 81.9 |
| | $\epsilon = 0.06$ | 10.1 | 20.2 | 43.8 | 72.6 |
| PGD | $\epsilon = 0.2$ | 5.6 | 7.7 | 78.7 | 87.4 |
| | $\epsilon = 0.4$ | 4.8 | 6.8 | 55.5 | 82.9 |

E. Number of Ensemble Members in ECN

For the 10-label classification problem, representing labels with unique codewords requires $N \geq 4$. Fig. 5 shows ECN’s performance as the number of ensemble members N increases. From $N = 4$ to $N = 10$, the testing accuracy under adversarial attacks grows rapidly and it starts to level out from $N = 10$ onwards. The performance saturation happens because for $N > 10$ any column in code matrix \mathbf{M} is a linear combination of the others so that it is inevitable for adversarial examples to transfer between ensemble members. Moreover, as N increases, the training time is (almost) linearly proportional to N . Hence, a lightweight individual network is advised to use.

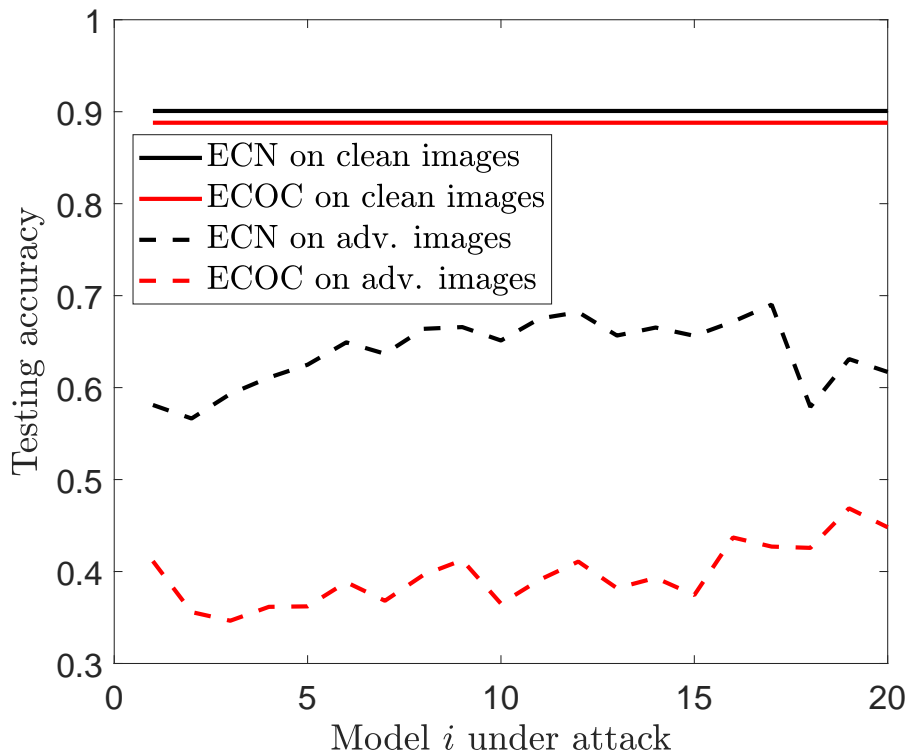


Fig. 4. Classification accuracy (%) on CIFAR10 examples where both ECN and ECOC use $N = 20$ binary classifiers and ECN uses net B as its binary classifier model and $\alpha = 10, \beta = 0$. The adversarial examples are generated by FGSM at $\epsilon = 0.04$.

TABLE VIII

CLASSIFICATION ACCURACY (%) ON ADVERSARIAL CIFAR10 EXAMPLES GENERATED BY FGSM AND PGD AT $\epsilon = 0.04$.

FOR ECN, WE USE $N = 10$ BINARY CLASSIFIERS AND SET $\alpha = 10, \beta = 0$.

| | No attack | | | FGSM | | | PGD | | |
|------|-----------|-------------|------------------|--------|-------|------------------|--------|-------------|------------------|
| | random | d_H | d_H & d_{VI} | random | d_H | d_H & d_{VI} | random | d_H | d_H & d_{VI} |
| mean | 88.9 | 88.9 | 88.9 | 48.1 | 51.4 | 51.8 | 40.44 | 46.48 | 46.63 |
| std. | 0.36 | 0.17 | 0.25 | 2.60 | 2.57 | 2.36 | 3.55 | 3.24 | 3.98 |

F. Row and/or Column Distance in Code Matrix

As indicated in (6), we generate a code matrix by jointly maximizing the Hamming distance between rows and the VI distance between columns. It will be interesting to see the impact of these two distance metrics on ECN. We consider three sets of code matrix:

- 1) random matrix whose entries are drawn randomly with probability 0.5 being 1 (or 0),
- 2) matrix with only the row distance $d_H(\mathbf{M})$ maximized while column distance $d_{VI}(\mathbf{M})$ is

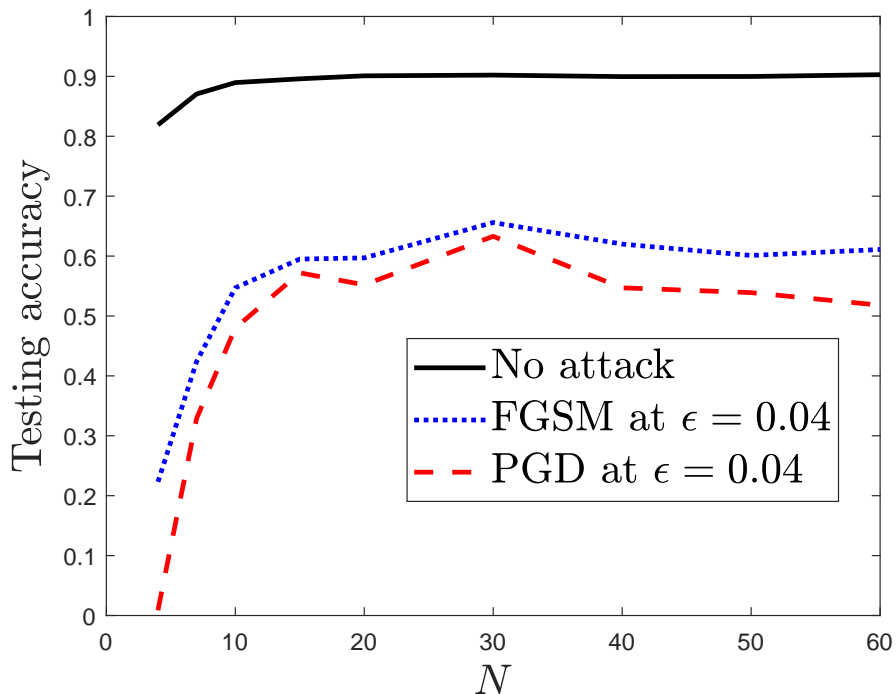


Fig. 5. Classification accuracy (%) on adversarial CIFAR10 examples using ECN_N where we use net B as the binary classifiers and change N from 4 to 60 and set $\alpha = 10, \beta = 0.5$. The adversarial examples are generated by FGSM and PGD both at $\epsilon = 0.04$.

left out in (6),

3) matrix with both $d_H(\mathbf{M})$ and $d_{VI}(\mathbf{M})$ maximized.

For each set, we independently generate 20 matrices. The code matrices in set 2 are designed to promote error tolerance while the code matrices in set 3 are designed to promote both error tolerance and model diversity. The statistic results are summarized in Table VIII. These three sets of code matrices make no difference in classifying the normal images. This is mainly because the trainable decoder in ECN will adapt itself to any code matrix so as to minimize the classification loss. Also, each binary neural network performs the binary classification problem with high accuracy. When classifying adversarial images, using random matrices in set 1 is noticeably worse than using those in set 2 and set 3 which means increasing error tolerance indeed improves the ECN’s robustness. On average using code matrices in set 3 gives the best adversarial testing accuracy. The improvement over set 2 seems not significant because we found the column distances in the matrices of set 2 are also reasonably large despite that only

TABLE IX

CLASSIFICATION ACCURACY (%) UNDER THE SAME SETTINGS AS IN TABLE VIII EXCEPT WE GENERATE CODE MATRICES IN THE FORM OF \mathbf{M}_b TO CONSTRUCT ECN_{10} .

| | No attack | FGSM | PGD |
|------|-----------|------|-------|
| mean | 86.8 | 44.2 | 33.02 |
| std. | 0.25 | 2.68 | 3.3 |

the row distance is optimized in set 2. To highlight the benefit of optimizing both row and column distances, we construct a code matrix $\mathbf{M}_b = [\mathbf{M}_a, 1 - \mathbf{M}_a]$ of size 10×10 where \mathbf{M}_a is generated by optimizing the row distance only. In this case, \mathbf{M}_b 's minimum VI distance between columns is 0 while its minimum Hamming distance between rows is still large. This means using \mathbf{M}_b to construct an ECN has poor ensemble diversity but good error tolerance. Comparing the results in Table IX with those under column d_H & d_{VI} in Table VIII, we see significant accuracy improvement by optimizing both row and column distances.

G. Generalization to q -ary ECN with $q \geq 2$

As we have discussed in Section III-B, our code matrix design allows $q \geq 2$. The q -ary ECN concatenates multiple q -ary classifiers in its encoder. We test $q = 3, 4$ and also includes $q = 2$ (binary) for comparison. The results in Table X indicate that increasing q reduces the adversarial robustness (except for C&W case). This is not unexpected because q -ary classifier has $q!$ possible outputs and the adversarial space grows as q increases, i.e., more output combinations adversary can mess up with less efforts.

TABLE X

CLASSIFICATION ACCURACY (%) ON ADVERSARIAL CIFAR10 EXAMPLES USING q -ARY ECN_{20} WITH $\alpha = 10, \beta = 0$.

| Attacks | Para. | $q = 2$ | $q = 3$ | $q = 4$ |
|---------|-------------------|---------|---------|---------|
| No att. | - | 90.1 | 90.7 | 90.7 |
| FGSM | $\epsilon = 0.04$ | 60.0 | 52.7 | 49.2 |
| BIM | $\epsilon = 0.04$ | 54.1 | 42.0 | 33.6 |
| PGD | $\epsilon = 0.04$ | 55.7 | 42.9 | 35.0 |
| JSMA | $\epsilon = 0.2$ | 78.9 | 76.3 | 51.6 |
| C&W | $\kappa = 1$ | 89.3 | 89.9 | 90.2 |

H. ECN using Sparse Code Matrix $\mathbf{M} \in \{-1, 0, +1\}^{L \times N}$

This is another generalization of ECN. The code matrix \mathbf{M} used to construct ECN is similar to 3-ary case as introduced in Section IV-G but we omit all examples in the training set for which $M(r, c) = 0$. This technique is inspired by [35] and makes it different from the $q = 3$ ECN discussed above. The sparse code matrix is selected from 100000 randomly generated matrix with the best metric introduced in [35], using the same way as in their experiments.

To adapt ECN to such code matrix, we make the following modifications.

- 1) **Encoder:** Each individual net f_n takes an input image x and outputs a scalar $f_n \in (-\infty, +\infty), \forall n = 1, \dots, N$.
- 2) **Decoder:** Stacking all individual nets' outputs into a vector $\mathbf{f}(x) = [f_1, \dots, f_N] \mathbb{R}^{1 \times N}$ and activating $\mathbf{f} \cdot \mathbf{M}^T \in \mathbb{R}^{1 \times L}$ by softplus function yields $\hat{\mathbf{y}} \in \mathbb{R}^{1 \times L}$

$$\hat{\mathbf{y}} = \log(1 + \exp(2\mathbf{f} \cdot \mathbf{M}^T)).$$

The row of \mathbf{M} that is the closest to \mathbf{f} leads to the largest entry of $\hat{\mathbf{y}}$. To normalize $\hat{\mathbf{y}}$ to probability distribution, we can apply softmax activation function on $\hat{\mathbf{y}}$.

We consider to use sparse code matrix as its behaviour mimics dropout layer but is more organized (unlike ignoring the neurons randomly as what dropout layer does).

From some initial experiments, we observe that with the same number of columns, ECN performs worse when using the sparse code matrix even in the no-attack case. This is because the sparse code matrix renders less information that the final decoder can adapt to. The classification accuracy is expected to improve with more columns. We leave this experiment in future work.

V. CONCLUSION

In this paper, we presented an ensemble model ECN which is inspired by ECOC and can be trained in end-to-end fashion. Designing a code matrix by optimizing both the Hamming distance between rows and VI distance between columns makes ECN more robust against adversarial examples than optimizing row Hamming distance alone. Combining ECN with other adversarial defenses such as adversarial training can further improve model robustness. We found including BNs makes ECN as well as other neural networks vulnerable to gradient-based adversarial attacks. We generalized ECN to allow its branches to be q -ary classifiers with $q \geq 2$ and found that q -ary ECN is less robust than the binary one. We showed how to construct ECN using sparse code matrix and studied its performance.

REFERENCES

- [1] A. Krizhevsky, I. Sutskever, and G. E. Hinton, “ImageNet classification with deep convolutional neural networks,” in *Proc. Advances Neural Inf. Process. Syst.*, 2012.
- [2] Y. Lecun, L. Bottou, Y. Bengio, and P. Haffner, “Gradient-based learning applied to document recognition,” *Proceedings of the IEEE*, vol. 86, no. 11, pp. 2278–2324, Nov 1998.
- [3] G. Hinton, L. Deng, D. Yu, G. E. Dahl, A. Mohamed, N. Jaitly, A. Senior, V. Vanhoucke, P. Nguyen, T. N. Sainath, and B. Kingsbury, “Deep neural networks for acoustic modeling in speech recognition: The shared views of four research groups,” *IEEE Signal Process. Mag.*, vol. 29, no. 6, pp. 82–97, Nov 2012.
- [4] D. Andor, C. Alberti, D. Weiss, A. Severyn, A. Presta, K. Ganchev, S. Petrov, and M. Collins, “Globally normalized transition-based neural networks,” in *Proc. Annu. Meeting Assoc. Comput. Linguistics*, 2016.
- [5] C. Szegedy, W. Zaremba, I. Sutskever, J. Bruna, D. Erhan, I. Goodfellow, and R. Fergus, “Intriguing properties of neural networks,” in *Proc. Int. Conf. Learning Representations*, 2013.
- [6] I. J. Goodfellow, J. Shlens, and C. Szegedy, “Explaining and harnessing adversarial examples,” in *Proc. Int. Conf. Learning Representations*, 2015.
- [7] N. Papernot, P. McDaniel, X. Wu, S. Jha, and A. Swami, “Distillation as a defense to adversarial perturbations against deep neural networks,” in *Proc. IEEE Symp. Security and Privacy*, 2016.
- [8] D. Hendrycks and K. Gimpel, “A baseline for detecting misclassified and out-of-distribution examples in neural networks,” in *Proc. Int. Conf. Learning Representations*, 2017.
- [9] D. Meng and H. Chen, “Magnet: a two-pronged defense against adversarial examples,” in *Proc. SIGSAC Conf. Comput. Commun. Security*, 2017.
- [10] P. Samangouei, M. Kabkab, and R. Chellappa, “Defense-GAN: protecting classifiers against adversarial attacks using generative models,” in *Proc. Int. Conf. Learning Representations*, 2018.
- [11] F. Liao, M. Liang, Y. Dong, T. Pang, X. Hu, and J. Zhu, “Defense against adversarial attacks using high-level representation guided denoiser,” in *Proc. Conf. Comput. Vision Pattern Recognition*, 2018.
- [12] A. Kurakin, I. Goodfellow, S. Bengio, Y. Dong, F. Liao, M. Liang, T. Pang, J. Zhu, X. Hu, C. Xie, J. Wang, Z. Zhang, Z. Ren, A. Yuille, S. Huang, Y. Zhao, Y. Zhao, Z. Han, J. Long, Y. Berdibekov, T. Akiba, S. Tokui, and M. Abe, “Adversarial attacks and defences competition,” in *arXiv preprint arXiv:1804.00097v1*, 2019.
- [13] T. Pang, K. Xu, C. Du, N. Chen, and J. Zhu, “Improving adversarial robustness via promoting ensemble diversity,” in *Proc. Int. Conf. Mach. Learning*, 2019.
- [14] T. G. Dietterich and G. Bakiri, “Solving multiclass learning problems via error correcting output codes,” *J. Artificial Intell. Res.*, vol. 2, no. 1, pp. 263–286, Aug. 1994.
- [15] N. García-Pedrajas and C. Fyfe, “Evolving output codes for multiclass problems,” *IEEE Trans. Evol. Comput.*, vol. 12, no. 1, pp. 93–106, Feb 2008.
- [16] T.-Y. Wang, Y. S. Han, P. K. Varshney, and P.-N. Chen, “Distributed fault-tolerant classification in wireless sensor networks,” *IEEE J. Sel. Areas Commun.*, vol. 23, no. 4, pp. 724–734, Apr. 2005.
- [17] C. Yao, P.-N. Chen, T.-Y. Wang, Y. S. Han, and P. K. Varshney, “Performance analysis and code design for minimum Hamming distance fusion in wireless sensor networks,” *IEEE Trans. Inf. Theory*, vol. 53, no. 5, pp. 1716–1734, Apr. 2007.
- [18] A. Vempaty, L. R. Varshney, and P. K. Varshney, “Reliable crowdsourcing for multi-class labeling using coding theory,” *IEEE J. Sel. Topics Signal Process.*, vol. 8, no. 4, pp. 667–679, Aug. 2014.
- [19] Q. Kang and W. P. Tay, “Sequential multi-class labeling in crowdsourcing,” *IEEE Trans. Knowl. Data Eng.*, vol. 31, no. 11, pp. 2190 – 2199, Nov. 2019.

- [20] J. Yosinski, J. Clune, Y. Bengio, and H. Lipson, “How transferable are features in deep neural networks?” in *Proc. Advances Neural Inf. Process. Syst.*, 2014.
- [21] Y. LeCun, C. Cortes, and C. J. C. Burges, “The mnist database of handwritten digits,” 1998.
- [22] A. Krizhevsky and G. Hinton, “Learning multiple layers of features from tiny images,” 2009.
- [23] A. Kurakin, I. J. Goodfellow, and S. Bengio, “Adversarial examples in the physical world,” in *Proc. Int. Conf. Learning Representations*, 2017.
- [24] A. Mađry, A. Makelov, L. Schmidt, D. Tsipras, and A. Vladu, “Towards deep learning models resistant to adversarial attacks,” in *Proc. Int. Conf. Learning Representations*, 2018.
- [25] N. Papernot, P. McDaniel, S. Jha, M. Fredrikson, Z. B. Celik, and A. Swami, “The limitations of deep learning in adversarial settings,” in *Proc. IEEE Eur. Symp. Security Privacy*, 2016.
- [26] N. Carlini and D. Wagner, “Towards evaluating the robustness of neural networks,” in *Proc. IEEE Symp. Security and Privacy*, 2017.
- [27] M. Meilă, “Comparing clusterings by the variation of information,” in *Proc. Annu Conf. Learning Theory*, 2003.
- [28] O. Pujol, P. Radeva, and J. Vitria, “Discriminant ecoc: A heuristic method for application dependent design of error correcting output codes,” *IEEE Trans. Pattern Anal. Mach. Intell.*, vol. 28, no. 6, pp. 1007–1012, Jun. 2006.
- [29] S. Kirkpatrick, C. D. Gelatt, and M. P. Vecchi, “Optimization by simulated annealing,” *Science*, vol. 220, no. 4598, pp. 671–680, May 1983.
- [30] A. Gamal, L. Hemachandra, I. Shperling, and V. Wei, “Using simulated annealing to design good codes,” *IEEE Trans. Inf. Theory*, vol. 33, no. 1, pp. 116–123, Jan. 1987.
- [31] A. Krizhevsky and G. Hinton, “Learning multiple layers of features from tiny images,” Tech. Rep., 2009.
- [32] K. He, X. Zhang, S. Ren, and J. Sun, “Deep residual learning for image recognition,” in *Proc. Conf. Comput. Vision Pattern Recognition*, 2016.
- [33] A. Galloway, A. Golubeva, T. Tanay, M. Moussa, and G. W. Taylor, “Batch normalization is a cause of adversarial vulnerability,” *arXiv preprint 1905.02161*, 2019.
- [34] G. Yang, J. Pennington, V. Rao, J. Sohl-Dickstein, and S. S. Schoenholz, “A mean field theory of batch normalization,” in *Proc. Int. Conf. Learning Representations*, 2019.
- [35] E. L. Allwein, R. E. Schapire, and Y. Singer, “Reducing multiclass to binary: A unifying approach for margin classifiers,” *J. Mach. Learning Res.*, vol. 1, no. Dec, pp. 113–141, Dec. 2000.